26th International Conference on Harbor, Maritime and Multimodal Logistic Modeling & Simulation, 006
21th International Multidisciplinary Modeling & Simulation Multiconference

2724-0339 © 2024 Topaj and Tarovik.
doi: 10.46354/i3m.2024.hms.006

Ship route planning in simulation models of Arctic transport systems

Alex Topaj[1*] and Oleg Tarovik[1,2]

[1]LLC Bureau Hyperborea, 6 Kavalergardskaya Str., Saint Petersburg,191015, Russia
[2]Krylov State Research Centre, 44 Moskovskoe shosse, Saint Petersburg, 196158, Russia

[*]Corresponding author. Email address: aleksandr.topazh@bureauhyperborea.ru

Abstract

Rapid development of Arctic shipping necessitates studying marine transport systems operating in the Arctic. This paper presents an approach to integrate intelligent ship route planning procedures into simulation models of Arctic transport systems. The approach is based on two logical components. The first one is a specially developed simplified ship transit model that uses the equivalent ice thickness and shaft power of a ship as the only input parameters. The second component is the original mathematical method for ship routing in nonhomogeneous and nonstationary medium. This method is a modification of a well-known isochrone-based algorithm incorporating the special heuristic rule to reduce the number of points in a wavefront and ensure computational efficiency. The method considers additional constraints, such as spatiotemporal zones of prohibited shipping and maximum voyage duration. Also, it allows to optimize shaft power and ship heading (bow- or aft-forward operation) together with ship trajectory. The paper presents the results of the case study that prove that the principal features of the proposed approach match the real practice of ice navigation. The presented numerical method for route optimization has good computational efficiency and can be implemented as a functional built-in module in complex simulation models of maritime logistics.

Keywords: Ship Routing; Ship Transit Model; Equivalent Ice Thickness; Simulation

1. Introduction

Simulation modeling plays an important role in the study of complex intermodal transport systems, in particular those operating in the Arctic. The principal processes that usually need to be considered when building such a domain model are the following (Terzi and Cavalieri, 2004):

- cargo flows, i.e. the dynamics of the needs of logistics hubs for the import of consumed cargoes and the export of produced ones. An interesting and non-trivial problem here is the forming the schedule of ship voyages to satisfy all the requirements in time (Lima et al.,2015);
- exploitation of port and coastal infrastructure, as well as ship operations in port (Dragović et al., 2016);
- operations of the support fleet and icebreakers;
- filling and emptying of shore storage facilities;
- environmental dynamics;
- operation of a cargo ship.

The latter process or sub-model relates to the movement of a cargo ship from the source point to its destination. Sometimes, especially in case of open water navigation, it can be simulated most simply, i.e., as a uniform motion along the shortest possible trajectory. The speed is assumed to be constant, and the total time can be determined by the total length of the traveled path. As a result, there is almost no variability in the voyage duration on the same cargo line during model running.

On the contrary, ice is a sufficiently heterogeneous and dynamic medium. Therefore, the duration and severity of a particular voyage are the main source of uncertainty in real Arctic transportation systems. Thus, it should be properly reflected in the model. It means that both optimal curvilinear route and variable speed regime of ship voyage caused by the severity of current environmental conditions should be taken into account in the sub-model related to ship movement.

Certainly, the route planning process, i.e., the search for the optimal path and speed regime of ship voyages is important not only in the simulation modelling; this task has an independent meaning and importance (Tran et al., 2023). It is closely related to many other specific problems, such as the development of ship performance model, weather and ice monitoring and forecasting,

accounting for navigation restrictions, etc.

Each of the mentioned issues forms a separate field of investigation. Mathematical methods of path finding and ship route optimization in ice are closely related to the general task of vehicle routing in a temporally and spatially varying environment. There are two basic approaches in this area (Jeong et al., 2019; Zis et al., 2020). The first one is associated with finding a path using a predefined grid or a graph. These are the methods of Dijkstra, A*, and dynamic programming (Wang et al., 2018; Wang et al., 2019; Zhu et al., 2016; Zaccone et al., 2018). The second one is the so-called cell-free or wave-based approach, which allows us to find a path in continuous space by constructing successive lines of equal levels of the optimization criterion, such as isochrones or isocosts (Szłapczyńska and Śmierzchalski, 2008; Wang et al., 2017).

Estimating the attainable ship speed for a given percentage of shaft power under specific environmental conditions is the responsibility of the ship performance model. There are a lot of corresponding studies (Kotovirta et al., 2009; Li et al., 2018) that differ from each other in the degree of detail in the description of the modelled processes, as well as in the number of input factors taken into account (both ice parameters and vessel parameters).

And finally, a serious and not yet fully resolved task is the regular supply of route planning services with actual and forecast data on ice conditions. Multispectral and radar satellite images are currently the main tool for monitoring the ice cover in the Polar Regions (Huang et al., 2024). Unfortunately, their processing does not yet permit to obtain an adequate understanding of many ice parameters that are of paramount importance for shipping, e.g., compression, hummocking, horizontal size of ice floes, ice cracks, and discontinuities of ice cover. In turn, the lack of accurate diagnostic ice maps makes it difficult to forecast the future ice dynamics, since the initial conditions for modeling dynamic processes are quite approximate.

Integration of the route planning algorithms into the business logic of simulation model imposes additional requirements on all the procedures listed above. The main requirement is the efficiency of corresponding computational algorithms. Indeed, the model always runs in accelerated time; it can simulate thousands of virtual voyages of ships during one simulation experiment. Thus, the built-in procedure for assigning the optimal route for each voyage should not significantly slow down execution of the model, and the simplest and the most effective methods to implement all the components of the route planning process should be applied. Author's efforts in development and practical use of corresponding solutions form the content of the presented paper. It is organized as follows: section 2 describes the methods used for the study (ship performance model, presentation of ice dynamics and routing algorithm itself), section 3 presents the selected results for the demonstrating case and their discussion, and section 4 concludes and finalizes the contribution.

2. Materials and Methods

2.1. Simplified ship performance model

The main advantage of the low-fidelity ship ice performance models is their simplicity, which makes them a useful tool in case when high-fidelity simulators are unavailable or impossible to implement due to the lack of input data.

In this study, we implemented a ship transit model based on the so-called icebreaking curve, which is quite simple and widely used in strategic simulations of the Arctic fleet. Such a curve directly connects ship speed v with the thickness of level ice h. By means of studying the icebreaking curves from full-scale ice trials and high-fidelity simulations, we obtained the Parabolic Icebreaking Curve Model (PICM) that builds an entire icebreaking curve based on two input variables:

V_{OW} – maximum attainable speed of a ship in open water, knots

H_{lim} – icebreaking capability of a ship in level ice, i.e. the maximum thickness of ice that allows ship movement in continuous mode with a speed V_{lim} equal to 2 knots (1 knot abbreviated later as "kn" is equal to 1.852 km/h).

The PICM model also considers the relative shaft power P as an additional variable. Unfortunately, a detailed description of obtaining such a model goes beyond the scope of this article, so only the final expression is given in Eq.(1).

$$v(h) = a_2 \cdot h^2 \cdot P^{n1} + a_1 \cdot h + a_0 \cdot P^{n2} \quad (1)$$

where

a_2, a_1 and a_0 are the coefficients of the parabolic curve:

$a_2 = V_{OW} \cdot (1-k)/{H_{lim}}^2$,

$a_1 = (V_{OW} \cdot (k-2) + V_{lim})/H_{lim}$,

$a_0 = V_{OW}$.

V_{lim} is a speed that corresponds to H_{lim} and usually assumed to be $V_{lim} = 2$ kn.

P is a relative shaft power that changes from 0 to 1.

$n1$ and $n2$ are the empiric coefficients that model the dependence of ship speed from P; during model validation the following values were obtained:

$n1 = 0.116$,

$n2 = 0.311$.

k is the empiric coefficient that defines deflection of the curve; model validation gave the following:

$k = 0.64$.

To maintain a realistic parabolic shape of an icebreaking curve, the following restriction of V_{lim} value must be met:

$$V_{lim} < 2 \cdot V_{OW} \cdot \left(1 - k/2 - \sqrt{1-k}\right) \quad (2)$$

Validation of the PICM model showed that it may be applied for both bow- and aft-forward modes of operation of double-acting ships.

Fig.1 gives an example of icebreaking curves of YamalMax LNG carrier for the bow- and aft-forward modes of operation built by PICM model and high-fidelity simulator. At the bow-forward mode, we assumed $V_{OW} = 21$ kn and $H_{lim} = 1.6$ m, while at the aft-forward $V_{OW} = 16.2$ kn and $H_{lim} = 2.2$ m.

As we can see from the comparison of PICM with the high-fidelity simulator, in this case, the accuracy is acceptable. If we consider the entire sample of Arctic vessels, which were used to validate the PICM model (12 ships of various dimensions and ice class), then for all points the standard deviation of the model prediction is 0.57 knots, while the expected value is close to zero; this proves the acceptable accuracy of the model.

Even though the PICM model relates to ship operation in level ice, its application in case of a simplified description of ice conditions in terms of equivalent ice thickness H_{EQ} is also possible. We may assume that instead of continuous level ice thickness h the model may get the thickness H_{EQ}, which reflects the overall complexity of ice for ship movement.

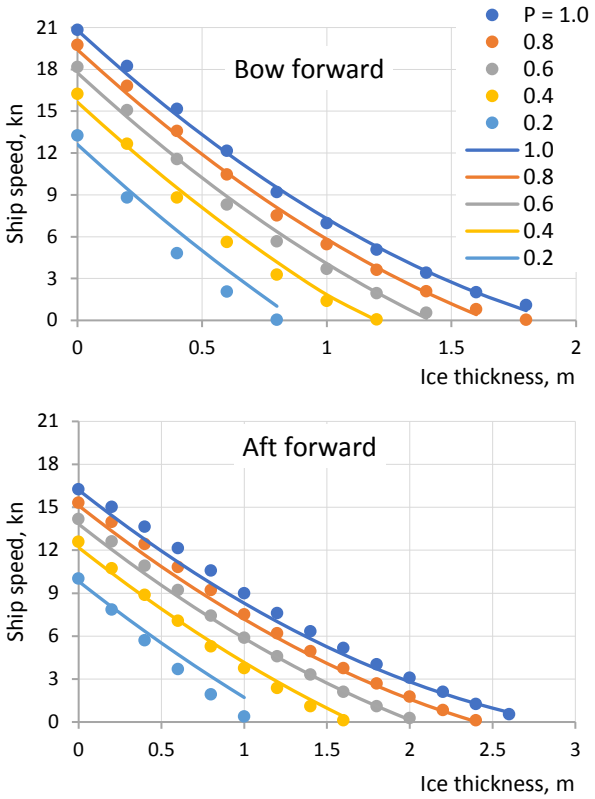

Figure 1. Icebreaking curves of YamalMax LNG carrier for the bow- and aft-forward modes of operation built by PICM model (lines) and high-fidelity simulator (dots).

2.2. Dynamics of ice conditions

The simplified ship performance model presented in section 2.1 uses so-called equivalent ice thickness as the only input data describing the environment. Such an approach averages all ice features of heterogeneous ice cover in the local area (ice concentration, thickness, hummocks, compression, etc.) into a single value of conventional ice thickness of virtual continuous level ice (or fast ice).

The fact that the spatial distribution of the severity of ice conditions can be described by the field of a single scalar variable is very convenient from the point of view of the simulation model. In this case, the dynamics of the environment can be simulated as a change of successive ice charts containing only one single ice parameter. To form such ice charts, the method of spatiotemporal stochastic generation of random scalar fields may be applied (May et al, 2023). The only difference is that the equivalent ice thickness is considered as a generated value instead of the ice concentration that was originally studied in (May et al, 2023).

There are various approaches and heuristics for convolving several parameters of ice cover having different nature into a single representative predictor of ship performance model (Milaković et al., 2020). In the current study, we use the original method, which is also described briefly due to restrictions of paper length.

When calculating the equivalent ice thickness H_{EQ} we considered all the parameters of ice that were available in the original dataset provided by the Arctic and Antarctic Research Institute (AARI).

$$H_{EQ} = k_{CT} \cdot (H_C + H_T + H_{SN}) \cdot k_{mon} \cdot k_D, \text{ cm} \quad (3)$$

where

$H_C = (C_1 \cdot S_1 + C_2 \cdot S_2 + C_3 \cdot S_3)/C_T$ is the average ice thickness by ice concentration,

C_1, C_2, and C_3 are the partial concentrations of three age gradations of ice,

S_1, S_2, and S_3 are the thicknesses of ice of three age gradations, cm,

$C_T = C_1 + C_2 + C_3$ is the total ice concentration in percent,

$H_T = 75(0.031T^2 + 0.125T - 0.156) \cdot (H_C/100)^{(1.07-0.07T)}$ is the addition to ice thickness due to the degree of hummocking T estimated using the national Russian scale (from 0 to 5), where one grade of hummocking approximately corresponds to 20% coverage of ice area with hummocks (Adamovich et al., 1995),

$H_{SN} = 0.5 \cdot (C_1 \cdot S_{SN1} + C_2 \cdot S_{SN2} + C_3 \cdot S_{SN3})/C_T$ is the addition to ice thickness due to snow cover,

S_{SN1}, S_{SN2}, S_{SN3} are the thicknesses of snow cover of ice of three age gradations, cm,

$k_{CT} = (C_T/100)^{2.5}$ is the empirical coefficient that considers total ice concentration,

$k_{mon} = -0.000107 \cdot M^4 + 0.00343 \cdot M^3 - 0.03 \cdot M^2 + 0.0515 \cdot M^2 + 1.07$ is the empirical coefficient that considers the change in ice cover strength depending on month number M,

$k_D = 0.1916 \cdot \ln(D_{ave}) - 0.2792$ is the empirical coefficient, which considers the average horizontal size (diameter) of ice floes D_{ave},

$0 \le k_D \le 1$,

$D_{ave} = (C_1 \cdot D_1 + C_2 \cdot D_2 + C_3 \cdot D_3)/C_T$,

D_1, D_2, and D_3 are the average diameters of three age gradations of ice.

To provide the input data for the case study described below we used a specially implemented database of historical ice observations and forecasts. Weekly digital ice charts are the main information source for this database (http://wdc.aari.ru/datasets) and were provided by the World Data Center of AARI for the period 1997-2022. These charts were created by the ice experts based on the analysis of satellite information and contain data about ice concentration, thickness, and form of ice (horizontal size) in SIGRID-3 format for three stages of ice development. Additionally, hummocking and melting stage were estimated according to the climate maps of their averaged distribution in the Arctic seas for the seasons with different severity of ice conditions. Ice compression was not considered in the case study, since weekly temporal resolution does not allow to capture the values of ice pressure. Several sequential chats representing the spatial distribution of equivalent thickness calculated by Eq.(3) were built for the season 2021-2022. They are shown as the background images in Fig. 4, where the gray-scale palette was used; black color corresponds to conventionally impassable ice with H_{EQ}>2.7 m (shore or shallows are also shown in black), while white color is the open water.

2.3. Routing algorithm

The developed mathematical method for ship route optimization is a significant modification and improvement of the earlier published author's algorithm (Topaj et al., 2019). In this study, we extend the traditional isochrone-oriented approach, where the main new idea is the new effective method for eliminating unpromising points at each step of the iterative algorithm of wave propagation. The method details are as following.

The entire working space (i.e., the area where the optimal route

from the starting point to the ending point can theoretically pass) is discretized by regular computational grid. The spatial resolution of such a grid is a matter for a separate study, but anyway, it must be more detailed than the spatial resolution of environmental conditions. It is necessary to note that the nodes of the selected grid are not used later as working points of the proposed algorithm. Therefore, not being "cell-free" in the full sense of the word, the proposed method remains a wave-based one.

At each stage of the iterative path finding algorithm, every cell of the grid has two sets of so-called reference points. The first set consists of the reference points for the current iteration (we denote these points below as P_i) and the second set contains the future reference points for the next iteration (P_{i+}).

Each reference point is characterized by the following attributes:

- Geographical coordinates (latitude and longitude). Reference point may lie in any location inside the parent cell
- Point status or its number *i* in the corresponding set. Status represents the current mode of vessel motion in the point, i.e., bow- or aft-forward. Later for definiteness, we consider only the case of independent movement of double-acting vessel in ice. So, we identify two possible statuses: 0 – independent motion bow-forward; 1 – independent motion aft-forward. In case of icebreaker assisted operation there could be the corresponding modes of ship movement with an icebreaker.
- *W* – integral cost of the point at the current step of iterative algorithm. It is the minimal cost that permits to achieve the point neighborhood at the current time period since the voyage start.
- Pointer to the parent point *p*, i.e. the point, which generated this particular point in the currently optimal route.
- *Q* – shaft power (or power mode) when moving from the parent point to this one along the currently optimal route.

Before the algorithm starts (at the zero iteration), all grid cells are assigned an initial set of reference points that are located in the cell center position and have the following attribute values: *W = Double.MaxValue, p=null, Q = 0* (similarly for the attributes of the points with the signs, i.e. for next iteration estimates). The only exception is the cell containing the starting point of the voyage. For this cell the reference point is located in the actual starting position, its status value equals to *0* and *W = 0*.

The first dynamic stage of proposed algorithm is the sequential (wave-analogue) propagation of optimal cost values along the computational grid. The time step of single iteration Δt is the parameter of algorithm, i.e., its temporal resolution. The algorithm for iterative recalculation of grid points attributes at step *k* consists of the following steps:

All current reference points with different statuses P_i for all grid cells are sequentially scanned. If the value *W* for the point is equal to *Double.MaxValue*, then it is considered unachievable for the moment and skipped. Otherwise, if for the current physical time $k{\cdot}\Delta t$ the point occurs in the prohibited zone, then its parameters are assigned to *W = Double.MaxValue, p=null, Q=0* (wave propagation terminates). Otherwise, a radial propagation procedure for the current point is carried out. Propagation distance is determined by the speed of movement corresponding to the selected percentage of shaft power, which moves from 0 (standing still) to 100% (maximum achievable speed under the given conditions). The number and the values of shaft power gradations, as well as the angular resolution of the course angle variation are the specific settings of the algorithm.

Calculation of the distance covered by a ship in a period Δt at a given shaft power in a heterogeneous environment can be done in two ways. The simplest approach is an explicit integration scheme. In this case, one multiplies the achievable speed in the starting point by the movement time Δt. Such an approach does not consider the possible change in external conditions along the trajectory. But for the regular computational grid, another approach is possible that involves a precise integration of elementary movement step. In this case, the total distance is the sum of individual paths that the ship passes in each grid cell. The length of each elementary part can be determined geometrically from the position of the starting point and the course angle. Since in each cell the external conditions are set as constant, the achievable speed and, accordingly, the time of movement inside the cell can also be calculated with absolute accuracy. Thus, for this case, the wave propagation distance in a given direction for a given shaft power is calculated as:

$$S(\alpha,\gamma,\Delta t,m)=\sum_j S_j\,,$$
$$\sum_j \Delta t_j=\Delta t \quad ; \quad \Delta t_j=\frac{S_j}{V_j(\alpha,\gamma,m,H_{EQ})}\,, \tag{4}$$

where α is the course angle, γ is the shaft power percentage, Δt is a time step, *m* is the status of the parent point, H_{EQ} is the equivalent ice thickness in j-th cell, and V_j is the achievable ship speed estimated by simplified ship performance model. Figure 2 demonstrates the procedure of discrete wave propagation from a single source point.

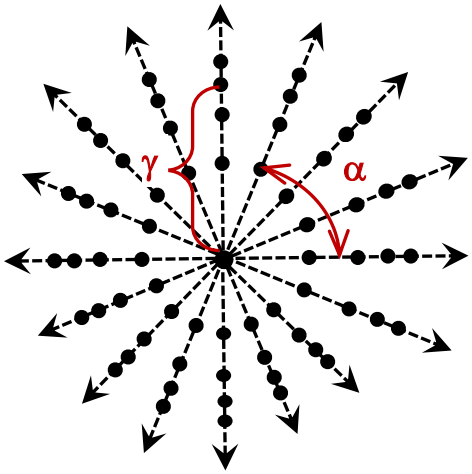

Figure 2. Generation of children reference point in wave propagation algorithm

Each parent point with a specific status can generate descendant points of all other statuses, but their attributes and coordinates may depend on the type of status transformation. The corresponding rules are described below.

The point P_0 generates:

- the set of points P_{0+}* at a distance $S(\alpha,\gamma,\Delta t,0)$ with value $W^*=W+F\cdot\Delta t+C_F\cdot R(\gamma)\cdot\Delta t$, $p^*=P_0$, $Q^*=\gamma\cdot Q_{max}$, where *F* is the ship freight rate of a ship, *R* is a fuel consumption rate for a given power, C_F is a fuel cost, Q_{max} is the maximum shaft power;
- the set of points P_{1+}* at a distance $S(\alpha,\gamma,\Delta t-t_r,1)$ with value $W^*=W+F\cdot\Delta t+C_F\cdot R(\gamma)\cdot\Delta t$, $p^*=P_0$,

$Q^* = \gamma \cdot Q_{max}$, where $t_r = t_r(H_{EQ})$ is the required rotation time of the ship in the current environment. Estimation of t_r for the modern high tonnage vessels having a significant circulation radius was done based on the results of Tarovik and Kazantsev (2022). We should note that the entire method remains valid only for the case when $t_r < \Delta t$.

In turn, any point P_1 generates:

- the set of points P_{1+}* at a distance $S(\alpha, \gamma, \Delta t, 1)$ with value $W^* = W + F \cdot \Delta t + C_F \cdot R(\gamma) \cdot \Delta t$, $p^* = P_1$, $Q^* = \gamma \cdot Q_{max}$;
- the set of points P_{0+}* at a distance $S(\alpha, \gamma, \Delta t - t_r, 0)$ with value $W^* = W + F \cdot \Delta t + C_F \cdot R(\gamma) \cdot \Delta t$, $p^* = P_1$, $Q^* = \gamma \cdot Q_{max}$.

The main idea of the proposed algorithm is that the unpromising reference points of the next generation are eliminated immediately. The rule of such elimination is trivial. The point is not generated if the target cell already contains the better reference point with the same status. Otherwise, the existing reference point with the same status in the target cell is removed and a new reference point is generated. Thus, any cell of the calculated grid always contains maximum two reference points of each status – one for the current generation and one for the next.

To find and to leave the best point in the cell, one needs to have the rule to compare the prospects of the points. Since the achieving time for all points in the current iteration is the same, we must take into consideration their two remaining features: costs W and locations inside the cell, i.e., the coordinates. We propose two alternative approaches to form the comparison rule for the reference points in the described routing algorithm. The simplest one is to consider only the cost. It means that we keep the cheapest point in every cell regardless of its location. A more sophisticated approach is presented in Fig. 3. Here, the supplementary price of covering an additional distance is added to or subtracted from the point cost for further comparison. This addition depends on the difference in orthodromic distances from both compared points to the endpoint.

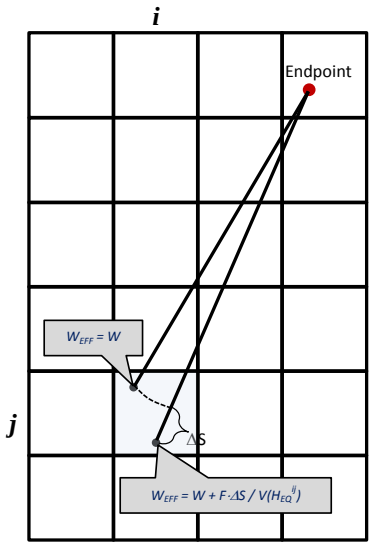

Figure 3. Calculation of the effective cost when comparing two generated reference points in one cell of the working grid.

After completion of the propagation procedure for all reference points, they are reassigned to all cells of the computation grid, i.e. $P_i = P_{i+}$; $P_{i+} = null$ and next step of the iterative algorithm starts.

Stage 1 of the propagation algorithm continues either until the endpoint's W value becomes less than *Double.MaxValue* (it means that finish point of the voyage becomes achievable in the fastest albeit very expensive way), or until the total number of iterations exceeds the arrival time limit. In the latter case, the routing problem is considered unsolvable.

Stage 2 starts when the value of W_F for any reference point in the cell containing the destination point F becomes less than *Double.MaxValue*. It means that we already can construct a certain valid and fastest route to reach the target in required time, but this path may not lead to minimal cost. Later, the permanent improvement of the route from the economic point of view takes place at each subsequent iteration.

At the second stage, the same actions are performed as at the first one, but there are additional possibilities to filter the set of considered potentially generating points. In particular, the following modifications are included in the computational scheme described above. In addition to the points where $W =$ *Double.MaxValue*, all points having $W > W^F - \frac{S^F}{V_{EC}} \cdot \left(F + R(Q_{EC})\right)$ are not considered as possible parents for cost propagation. Here S^F is the straight orthodromic distance from the current point to the endpoint of the route, V_{EC} and Q_{EC} are the economical speed and economical power of the vessel in open water. In other words, we exclude from consideration all points that are guaranteed not to improve the already found route.

Stage 2 continues until one of two conditions is met:

- the next iteration corresponds to the time, which exceeds the time limit (possible voyage duration),
- none of the points (cells) generates the new descendants due to its priori estimated futility.

After the iterative algorithm stops the optimal route is formed in a backward mode, i.e., from child to parent points, starting from the cheapest reference point in the endpoint cell. Each route segment in addition to its length and direction will contain information about the power percentage and the mode of vessel movement.

3. Results and Discussion

Fig. 4 presents the results of the route planning for the selected case voyage. The route was built for the Yamalmax LNG carrier sailing from Murmansk (green point) to Pevek (red point) with a start date of 02/01/2022 and a maximum voyage duration of 25 days.

The maps on the left side illustrate the process of isochrones propagation for different iterations of the search procedure described in section 2.3. The green points are the reference points having status 0 (bow forward mode), the blue ones are the reference points corresponding to aft forward movement. Reference points for the cells of the computational grid that are still unattainable are marked in red.

Right side images are the selected steps demonstrating obtained optimal route in the dynamics of environmental change. Here the thickness of the route line shows the percentage of the shaft power, while the color of the line indicates the mode of movement (green is a bow-, and blue is the aft-forward mode).

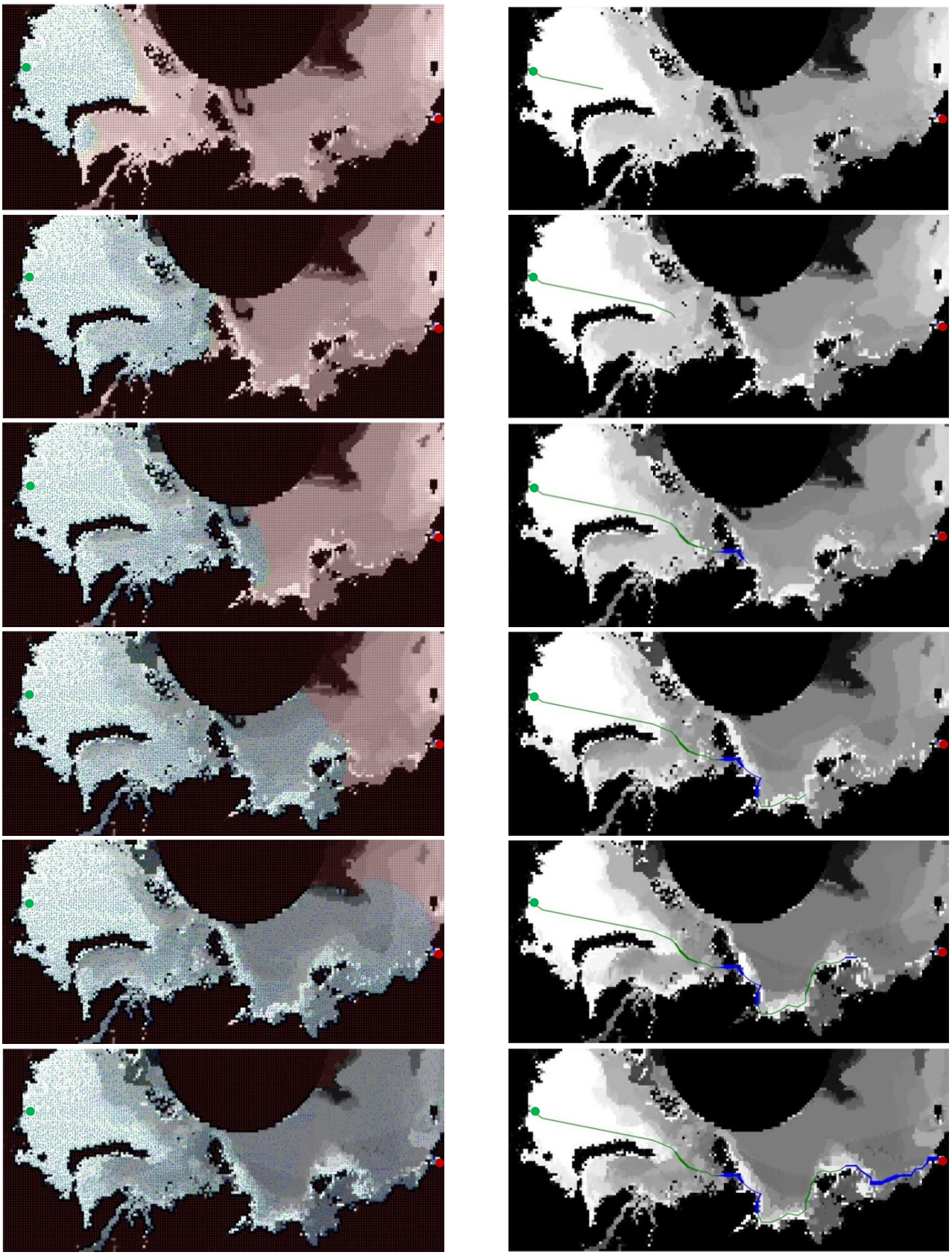

Figure 4. Dynamics of iterative search procedure and obtained optimal route

One can see that the route obtained by the proposed algorithm looks reasonable and has the following features:

- the recommended trajectory differs significantly from the shortest path that consists of orthodromic sections. The optimal route tries to use the large polynyas and areas of thinner ice located close to the shoreline;
- optimal route is formed based on the knowledge about the future state of ice, i.e. ice forecasts. In particular, one can see in the route animation that at certain moments the ship begins to slow down, waiting for the appearance of a promising water opening predicted by the next ice map;
- model ship effectively uses the ability to move aft-forward in sections of rather heavy ice when ice performance becomes more important. Moreover, the fact that turnaround of a ship requires a certain time leads to rather long sections of ship movement under a specific heading;
- estimated time of arrival (i.e. the voyage urgency) significantly affects the recommended power mode. If the ship has sufficient time reserve, its movement through open water and thin ice usually occurs in an economical mode. In the average-thick and in thick ice, the power plant operates in forced regimes.

The listed features of the obtained recommended route plan correspond to the real best practice of ice navigation, which indirectly proves the adequacy of the statement and solution of the considered problem.

4. Conclusions

This study presents two efficient solutions to introduce intellectual procedures of vessel route planning into the simulation models of Arctic transport systems. The first one is a simplified ship performance model that uses the equivalent ice thickness and shaft power of a ship as the only input parameters. The second one is the original mathematical method for ship routing in nonhomogeneous and nonstationary medium. It retains all the advantages of the previously published cell-free approach (Topaj et al., 2019). They are the possibility of free movement in an arbitrary direction, as well as the break in the trajectory at arbitrary points of space, not just at the predetermined ones. Accordingly, the problem of Manhattan Distance is absent under such an approach. But the computational grid is also used here as in the cell-based methods. Such a grid is needed for the heuristic algorithm to reduce the number of points in a wavefront.

Additionally, the proposed modification allows three important problems to be resolved compared to the previous version of the method:

- avoiding spatiotemporal zones of prohibited shipping,
- optimizing the shaft power mode together with the trajectory,
- considering the constrained voyage time.

Finally, a few words could be said regarding the computational efficiency of the described algorithms. A simplified ship transit model practically does not slow down the speed of the simulation model run. The proposed routing algorithm looks also rather fast in comparison with alternative traditional approaches. However, its speed is still insufficient for direct implementation into the logic of a simulation model where simultaneous planning of many voyages can take place. The latter seems to be the main limitation of the proposed algorithm. The following compromising solutions can be considered to overcome such limitation. Firstly, all possible vessel voyages can be planned a priory for an enlarged graph of routes of the Northern Sea Route. The route of each vessel on each edge of the graph and for each ice chart is pre-calculated in batch mode and then played out during the simulation model running. Such an approach has shown its effectiveness in several practical studies carried out by the authors. The second possible solution could be the parallelization of calculations, especially since the algorithmic structure of the proposed algorithm allows this to be done in a natural and easy way.

Funding

This study is supported by a grant from the Russian Science Foundation, Project No. 23-19-00039 “Theoretical foundations and applied instruments to develop a system for intelligent fleet planning and decision support in the Arctic shipping”.

References

Adamovich, N.M., Buzuyev, A.Ya., Fedyakov, V.E. (1995) The empiric model of vessel movement in the ice and generalization of the experience of the model usage in hydrometeorological support of shipping in the Arctic. Proceedings of POAC-1995, Murmansk, Russia, vol. 2, pp 30-40

Dragović B., Tzannatos E., Park N.K. (2016) Simulation modelling in ports and container terminals: literature overview and analysis by research field, application area and tool. Flexible Services and Manufacturing Journal, 29(1): 4–34, https://doi.org/10.1007/s10696-016-9239-5

Huang W., Yu A., Xu Q., Sun Q., Guo W., Ji S., Wen B., Qiu C. (2024) Sea Ice Extraction via Remote Sensing Imagery: Algorithms, Datasets, Applications and Challenges. Remote Sensing. 16(5):842. https://doi.org/10.3390/rs16050842

Jeong S.Y., Kang K.J., Kim H.-S., Kim J.-J., Roh M.-I. (2019) A Study of Ship Voyage Planning in the Northern Sea Route. Proc. of the 13th Pacific-Asia Offshore Mechanics Symposium, pp. 579–584.

Kotovirta V., Jalonen R., Axell L., Riska K., Berglund R. (2009) A system for route optimization in ice-covered waters, Cold Regions Sciience and Technology (55): 52–62, https://doi.org/10.1016/j.coldregions.2008.07.003

Li F., Goerlandt F., Kujala P., Lehtiranta J., Lensu M. (2018) Evaluation of selected state-of-the-art methods for ship transit simulation in various ice conditions based on full-scale measurement. Cold Regions Science and Technology, (151): 94-108, https://doi.org/10.1016/j.coldregions.2018.03.008.

Lima A. D. P., Werner de Mascarenhas F., & Frazzon E. M. (2015). Simulation- Based Planning and Control of Transport Flows in Port Logistic Systems. Mathematical Problems in Engineering, 2015(1), 862635, https://doi.org/10.1155/2015/862635

May, R.I., Guzenko, R.B., Tarovik, O.V. et al. (2023). Stochastic Modeling of Sea Ice Concentration to Assess Navigation Conditions along the Northern Sea Route. Izv. Atmos. Ocean. Phys. 59 (Suppl 1), S57–S69 https://doi.org/10.1134/S0001433823130091

Milaković, A. S., Li, F., von Bock und Polach, R. U. F., Ehlers, S. (2020). Equivalent ice thickness in ship ice transit simulations: overview of existing definitions and proposition of an improved one. Ship Technology Research, 67(2), 84–100.

https://doi.org/10.1080/09377255.2019.1655260.

Szłapczyńska J. and Śmierzchalski R. (2008) Adopted isochrones method improving ship safety in weather routing with evolutionary approach, Reliabil. Risk Anal. Theory Appl. (2): 139–145.

Terzi S. and Cavalieri S. (2004). Simulation in the supply chain context: a survey. Computers in Industry, 53(1): 3–16, https://doi.org/10.1016/S0166-3615(03)00104-0

Tarovik O.V. and Kazantsev M.A. (2022) Estimation of the turning maneuver duration of double acting ships in ice using navigation simulation. Research Bulletin by Russian Maritime Register of Shipping, 68/69, 4-19 (In Russian).

Topaj A.G., Tarovik O.V., Bakharev A.A., Kondratenko A.A. (2019) Optimal ice routing of a ship with icebreaker assistance. Applied Ocean Research. 86, 177-187. https://doi.org/10.1016/j.apor.2019.02.021

Tran T. T., Browne T., Musharraf M., Veitc B. (2023). Pathfinding and optimization for vessels in ice: A literature review. Cold Regions Science and Technology, (211), 103876. https://doi.org/10.1016/j.coldregions.2023.103876

Wang H., Mao W., Eriksson L. (2019) A Three-Dimensional Dijkstra's algorithm for multi-objective ship voyage optimization. Ocean Engineering, (186), 106131, https://doi.org/10.1016/j.oceaneng.2019.106131

Wang H., Li P., Xue Yu., Korovkin M.V. (2017) Application of Improved Isochron Method in Ship's Minimum Voyage Time Weather Routing. Vestnik Sankt-Peterburgskogo Universiteta, Prikladnaya Matematika, Informatika, Protsessy Upravleniya, (13):286–299, (In Russian) https://doi.org/10.21638/11701/spbu10.2017.306

Wang Y., Zhang R., Qian L. (2018) An improved A* algorithm based on hesitant fuzzy sets theory for multi-criteria arctic route planning. Symmetry (10): 765, https://doi.org/10.3390/sym10120765

Zaccone R., Ottaviani E., Figari M., Altosole M. (2018) Ship voyage optimization for safe and energy-efficient navigation: A dynamic programming approach, Ocean Engineering, (153): 215-224, https://doi.org/10.1016/j.oceaneng.2018.01.100.

Zhu X., Wang H., Shen Z., Lv H. (2016) Ship weather routing based on modified Dijkstra algorithm, Proc. of MMEBC 2016 6: 696–699, https://doi.org/10.2991/mmebc-16.2016.147.

Zis T. P. V., Psaraftis H. N., Li D. (2020). Ship weather routing: A taxonomy and survey. Ocean Engineering, (213), p.18. https://doi.org/10.1016/j.oceaneng.2020.107697